

How dependent is climate change projection of Indian summer monsoon rainfall and extreme events on model resolution?

K. Rajendran^{1,*}, S. Sajani¹, C. B. Jayasankar¹ and A. Kitoh²

¹CSIR–Fourth Paradigm Institute (CSIR–4PI), Bangalore 560 037, India

²Meteorological Research Institute, Tsukuba, Japan

Advances in climate modelling now provide the opportunity for utilizing global general circulation models (GCMs) at very high-resolution for projections of future climate and extreme events. Diagnostics of global atmospheric GCM simulations at different horizontal resolutions of 20, 60, 120 and 180 km reveals the marked skill of 20 km mesh GCM (MRI-AGCM3.2S) in capturing regional characteristics of climatological summer monsoon rainfall over India and its frequency distribution, and mean annual variation of rainfall over most of the homogeneous regions of India. Future projections by time-slice simulations of MRI-AGCM3.2S under global warming scenario show widespread but spatially varying increase in rainfall over interior regions of peninsular, west central, central northeast and North East India (~5–20% of seasonal mean) and significant reduction in orographic rainfall over the west coast (~10–15%, consistent with the recent observed trends). MRI-AGCM3.2S projects spatially heterogeneous increase in warm days and extreme hot events (highest decile) over India. Projected changes in extreme rainfall events (above 95 percentile) show intensification of extreme rainfall over most parts of India by the end of the century with opposite change over the west coast. Ultra-high-resolution is found to be crucial not only for realistic mean summer monsoon simulation, but for achieving useful future projections of Indian monsoon and extremes. At lower resolution, the simulations fail to capture the observed characteristics of present-day monsoon rainfall and its spatial heterogeneity, and projections lack useful regional climate information. Thus, consideration of fine-scale processes are critical for reasonable probabilistic projection of regional-scale climate change.

Keywords: Climate change projection, extreme events, general circulation model, ultra-high resolution.

Introduction

PROJECTIONS of changes in climate and extremes are critical for assessing potential impact of climate change

on human and natural systems. For example, in a predominantly agrarian society like India, agriculture is decided to a great extent by both weather (heavy rainfall, hot/cold events) and climate (duration and strength of seasonal rainfall) conditions. Global warming may precariously affect agricultural production and the livelihood of farmers by unpredictably changing the abundance of seasonal rainfall and extreme events. Thus, reliable projections of future climate change and changes in extreme events are crucial for agro-economic states of India. But the large inter-model difference in the simulation of Indian summer monsoon by the current global general circulation models (GCMs) and their low skill in simulating the present-day Indian summer monsoon variability¹ are the major detrimental factors.

Future climate projections indicate that summer precipitation is likely to increase in South Asia on a broader scale² and an increase in the frequency of intense precipitation events in parts of South Asia is also likely³. However, large uncertainty exists in projections of Asian monsoon precipitation⁴. GCMs often fail to capture the fine-scale structures that affect regional climate due to their coarse resolution. This aspect partially accounts for the deficiencies shown by GCMs in reproducing important aspects of the regional distribution of the Indian summer monsoon rainfall. It is known that the summer monsoon precipitation over the Indian subcontinent involves high-resolution processes of interaction between the large-scale monsoon circulation and local complex terrain, heterogeneous land surfaces, and adjacent warm oceans. So it is important to employ high-resolution models and understand the sensitivity of monsoon simulation to model resolution.

Employing very high-resolution global GCM can resolve features on finer spatial scales such as the Western Ghats^{5,6}. However, even the highest resolution simulation among Intergovernmental Panel for Climate Change Fourth Assessment Report (IPCC AR4) coupled models showed lack of reasonable fidelity in capturing important features of present-day summer monsoon rainfall³. This implies the significance of suitable physics schemes to be used in high-resolution models for achieving realistic monsoon simulation. Models with improved

*For correspondence. (e-mail: rajendrank@hotmail.com)

physics schemes, especially for parameterized deep convection, are found to markedly improve monsoon simulation⁷. Hence, it is meaningful to examine the role of model resolution in the presence of suitable deep convection schemes, on simulation and projection of Indian monsoon rainfall with focus on its regional characteristics. It is also pertinent to study the projected changes in high percentile (extremes) precipitation and temperature events under global warming using model configurations which have high fidelity for seasonal monsoon rainfall. In this article, we analyse the changes in mean monsoon precipitation and extreme temperature and precipitation events due to global warming and their sensitivity to model resolution and deep convection parameterization, using time-slice simulations of a global GCM by employing four resolutions and two deep convection parameterizations.

Model configurations, simulations and datasets

The model used for global warming projection is a global atmospheric GCM jointly developed by Japan Meteorological Agency (JMA) and Meteorological Research Institute (MRI), Japan^{5,8}. The model includes the Arakawa–Schubert cumulus parameterization scheme⁹ (hereafter referred to as AS) with a prognostic closure¹⁰. At the highest resolution, the model corresponds to triangular truncation 959 with a linear Gaussian grid ($T_L 959L60$) in the horizontal (the transform grid uses 1920×960 grid cells with approximate grid size of 20 km). The linear grid adopted in the model using a semi-Lagrangian scheme can suppress the aliasing effect arising from the quadratic Eulerian advection terms in addition to reducing the number of grid points¹¹. The model has 60 layers in the vertical, with the model top at 0.1 hPa. The simulation at this resolution is hereafter referred to as MRI-AGCM3.1S. To study simulation sensitivity to model resolution, three additional simulations of the model were performed at three lower resolutions of $T_L 319L60$ (~60 km grid size with 60 vertical layers), $T_L 159L40$ (~120 km grid size with 40 vertical layers) and $T_L 95L40$ (~180 km grid size with 40 vertical layers) using the same boundary forcing (hereafter referred to as MRI-AGCM3.1H, MRI-AGCM3.1M and MRI-AGCM3.1L respectively).

The higher resolution configurations (MRI-AGCM3.1S and MRI-AGCM3.1H) of the model¹² were integrated with a new deep convection scheme¹³ by Yoshimura (hereafter referred to as YS). The YS scheme is based on Tiedtke¹⁴ with modifications to represent all top-level cumulus plumes by interpolating two convective updrafts with maximum and minimum rates of turbulent entrainment and detrainment. The YS scheme in the model is found to yield a more realistic simulation of tropical precipitation¹². Both simulations have 64 vertical layers

with the top at 0.01 hPa (ref. 12). Hereafter, these simulations are referred to as MRI-AGCM3.2S and MRI-AGCM3.2H respectively.

Two cases of 25-year simulations for the present-day (1979–2003) and future (2075–2099) corresponding to the IPCC Special Report on Emissions Scenarios (SRES) A1B scenario¹⁵ are performed for each model configuration. For the present-day climate (PDC) simulation, observed sea-surface temperature (SST) and sea-ice concentration (SIC) from the Hadley Centre HadISST dataset¹⁶ for 1979–2003 are prescribed. The SST and SIC boundary conditions for the projected future climate (PFC) time-slice experiment are estimated^{5,17,18} using the Coupled Model Intercomparison Project phase 3 (CMIP3)¹⁹ multi-model SST data. Using the outputs of SST and SIC from different CMIP3 models, the estimation method uses a multi-model ensemble technique to incorporate the effects of future climate change along with realistic present-day interannual variability.

The validation data for the present-day rainfall simulations are taken from the daily India Meteorological Department (IMD) gridded rainfall data on $0.5^\circ \times 0.5^\circ$ grid for the period 1979–2007 (ref. 20). For rainfall validation, we have also used the Asian Precipitation Highly Resolved Observational Data Integration Towards Evaluation (APHRODITE) precipitation dataset from 1951 to 2007 on $0.25^\circ \times 0.25^\circ$ grid²¹.

Resolution impact on mean monsoon simulation

The fidelity of the model in representing the present-day climatological features of Indian monsoon is crucial for building confidence in its future projections. Over India, summer monsoon rainfall is mainly associated with the seasonal location of planetary scale Inter-Tropical Convergence Zone (ITCZ), which is significantly modulated by regional characteristics such as orography, convective processes influenced by geography and surrounding warm oceans. Due to the complex interaction among various processes, there are multiple locations for the seasonal tropical convergence zones (TCZs) or rainbelts to occur over the Indian region in summer¹. Hence, realistic incorporation of all these regional processes at sufficiently high-resolution in a global GCM is essential to achieve a reasonable mean summer monsoon rainfall simulation.

Summer monsoon rainfall

The most important aspect of Indian summer monsoon and the most difficult parameter for the GCMs to simulate is the rainfall occurring in the season¹. Figure 1 reveals numerous regional details of the summer mean (June–September average, referred to as JJAS) rainfall over India based on two different observations (APHRODITE rainfall and IMD rainfall for the period

1979–2003). The boundaries of six homogeneous regions of India²², viz. peninsular India (I), west central India (II), northwest India (III), hilly regions of India (IV), central northeast India (V) and North East (NE) India (VI) are also depicted. The major rainfall centres include meridionally oriented orographic maximum along the west coast of the Indian peninsula, relative maxima over the central Indian region, parts of the Indo-Gangetic Plain and the NE region. The narrow west coast orographic region has two distinct topographical and climatic features: to the west lies a coastal plain with heavy rainfall (windward side) and to the east lies a plateau with less rainfall (leeward side). The moisture-laden monsoon winds cause heavy rainfall on the windward side of the range, distinguishing it from the much drier leeward side. Most of the west coast rainfall (90%) occurs during June–September, there being comparatively less rainfall during the rest of the year. This illustrates the requirement for

ultra-high resolution in GCMs to provide important regional characteristics, especially in the context of orographic precipitation. There is a close comparison between the two datasets in representing the prominent features of summer mean rainfall and its spatial gradient over India.

The MRI-AGCM3.1S captures many aspects of the regional distribution of observed rainfall, especially the rainfall over parts of core monsoon region of west central and central northeast regions. On the southeast part of Peninsular India and northwest India, precipitation is relatively weak as in observation. However, there is a slight rainfall underestimation over southeastern parts of central northeast India around West Bengal. In comparison, all lower resolution simulations fail to represent the west coast orographic rainbelt and rainfall over NE India and the hilly regions. In terms of intensity, location and extent of the major rainbelts and relative distribution of high and low rainfall, MRI-AGCM3.1S tends to give improved simulation, especially over the west coast NE and hilly region of India. Regional details of rainfall over core monsoon zone are also close to observation in MRI-AGCM3.1S. Accordingly, the pattern correlation coefficient (PCC) against IMD mean rainfall increases to 0.78 in MRI-AGCM3.1S from 0.34 in MRI-AGCM3.1H (insignificant for MRI-AGCM3.1M and MRI-AGCM3.1L). The improvement in the simulation of east Asian summer monsoon by a 20 km model, in comparison to a lower resolution (~180 km) model, was brought out by the study of Kitoh and Kusunoki²³. Their study revealed that the high-resolution model was superior in simulating Baiu frontal structure, Baiu rainfall and the orographic rainfall qualitatively and quantitatively.

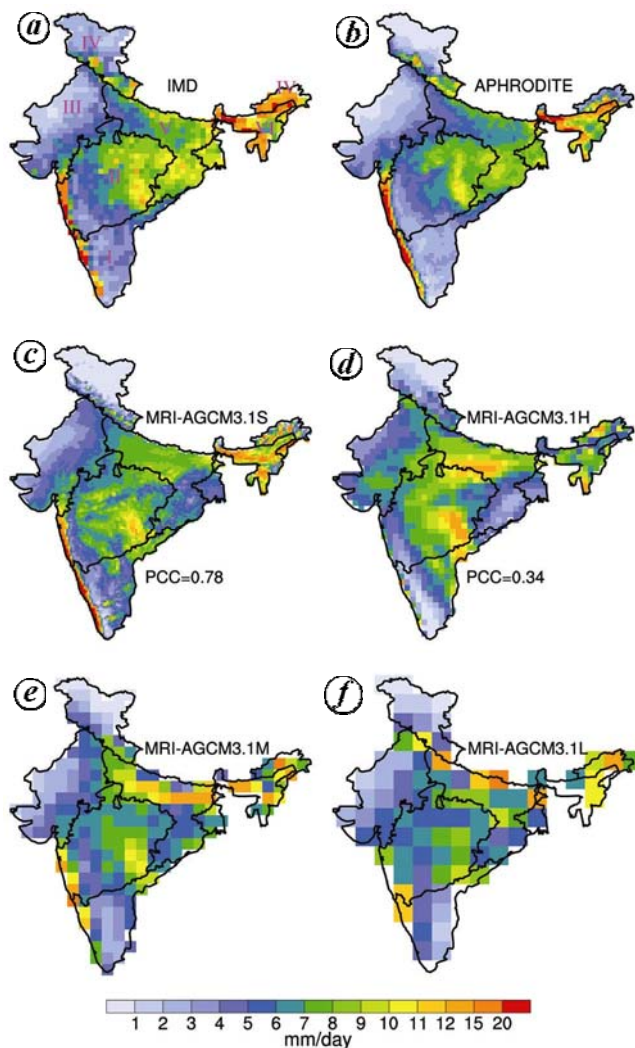


Figure 1. JJAS mean rainfall over India (mm day^{-1}) from IMD (a), APHRODITE (b) and PDC simulations with AS deep convection scheme at four resolutions: MRI-AGCM3.1S (c), MRI-AGCM3.1H (d), MRI-AGCM3.1M (e) and MRI-AGCM3.1L (f).

Sensitivity to deep convection parameterization

Figure 2 illustrates the impact of deep convection on seasonal mean monsoon from the two high-resolution simulations of MRI-AGCM3.2S and MRI-AGCM3.2H. When new YS deep convection scheme is used, there is a marked improvement in the simulation of rainfall over core monsoon region comprising west central India, central northeast India, NE India and the Hilly regions. The relative minima over southeast peninsular India and northwest India also become conspicuous and PCC increases to 0.81 for MRI-AGCM3.2S (0.75 for MRI-AGCM3.2H). With the new scheme, the west coast rainbelt is well represented in MRI-AGCM3.2H. The apparent improvement with YS scheme indicates that with optimum high-resolution of 20 km, further improvements in physics schemes could yield better simulation with quasi-realistic seasonal mean monsoon rainfall.

Frequency distribution of regional rainfall

Figure 3 shows the frequency distribution of JJAS rainfall over three important regions of peninsular India, west

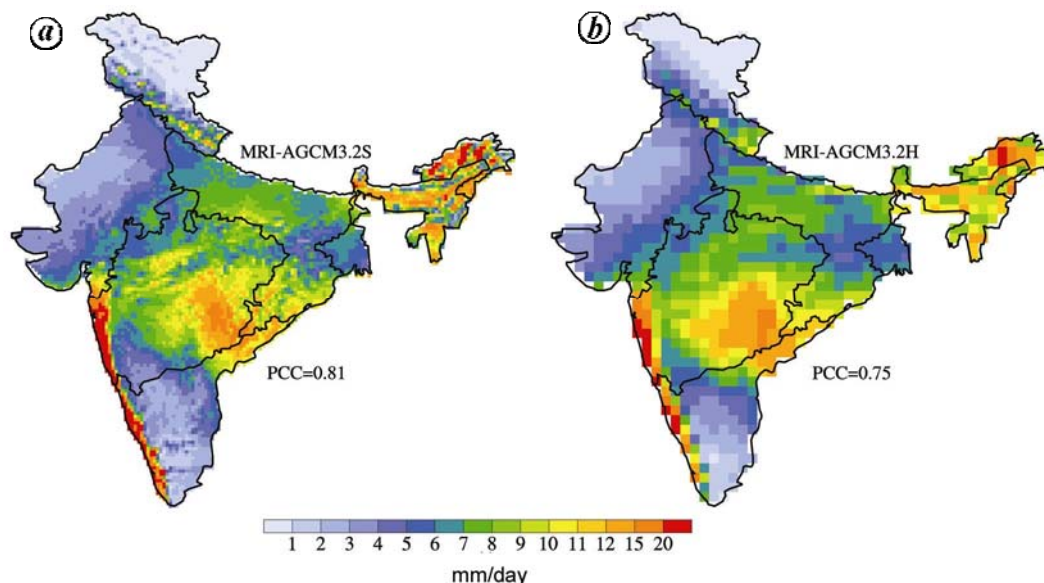


Figure 2. Same as Figure 1, but for PDC simulations of the model with YS deep convection scheme for MRI-AGCM3.2S (a) and MRI-AGCM3.2H (b).

central India and central northeast India (regions I, II and V). Despite slight quantitative difference between IMD rainfall and APHRODITE estimates, their modal structure is similar over all regions. There is a clear improvement in the simulation of rainfall distribution with YS scheme for region I, where MRI-AGCM3.2S simulation is the closest to observations. For region II, the new scheme helps to make the peak amplitudes comparable though they are shifted to higher rainfall by 3 mm/day. For region V, there is a marginal improvement in the distribution. With YS scheme, the model tends to have a better simulation of rainfall distribution, especially over core monsoon region.

Annual variation of homogeneous region rainfall

The primary manifestation of Indian monsoon which is crucial for an accurate simulation of the mean monsoon and its variability¹, is the annual variation with distinct seasonality in precipitation. Mean rainfall annual cycles for homogeneous regions of India from IMD observation and high-resolution PDC simulations are shown in Figure 4. Over all regions, except the hilly regions, there is marked seasonality in observed precipitation associated with the summer monsoon. The sudden enhancement in monthly precipitation associated with the onset phase, persistence of intense rainfall during June to September and the sharp reduction after the withdrawal in September are well manifested in observation and simulated by the models. The model shows reasonable skill in capturing the phases of rainfall annual variation with some quantitative differences. In some cases, simulations show a tendency for overestimating the mean rainfall and MRI-AGCM3.2S

simulation is able to bring down this anomaly (e.g. regions I–III).

Observed and simulated mean, standard deviation, and PCC (table in Figure 4) for different regions show that over peninsular India (region I) and northwest India (region III), YS scheme makes the summer mean and variability of rainfall closer to observation. For west central India (region II), the new scheme improves the variability (with a slight overestimation in mean rainfall), but sensitivity to higher resolution appears to have contributed towards improved spatial distribution (higher PCC). For regions V and VI, MRI-AGCM3.2S still has some deficiency as can be seen from the low PCCs for all the simulations. Overall, there are noticeable improvements in the simulation of mean, variability and annual variation of regional rainfall in MRI-AGCM3.2S.

Ultra-high resolution climate change projections

At the end of the 21st century, under global warming scenario (A1B), ultra-high-resolution models (MRI-AGCM3.2S and MRI-AGCM3.1S) predict (Figure 5) widespread but spatially varying increase in rainfall over the interior regions of peninsular, west central, central northeast and northeast India (~5–20% of seasonal mean). However, over the west coast of India (~10–15%), and some parts of northwest India and Jammu-Kashmir (~5–10%), future reduction in rainfall is projected by MRI-AGCM3.2S. Over the windward side of the west coast, the projected changes indicate significant weakening of rainfall in future. In the leeward side, increase in future rainfall is predicted by the model. These projected changes are qualitatively similar to the recent trends

observed over this region⁶. Rajendran *et al.*⁶ showed that drastic reduction of vertical ascent and weakening of circulation (increased stability) due to upper tropospheric warming effect predominate over the moisture build-up effect (that causes enhanced rainfall over the interior regions) in reducing rainfall over the west coast. In contrast, sustained increase in moisture transport into the interior region along with increased precipitable water causes intensification of future rainfall over northern parts of the west coast⁶.

So far, future scenarios for Indian summer monsoon rainfall even using high-resolution regional climate models projected relatively uniform climate change³. Spatial distribution of summer monsoon precipitation change due

to global warming shows larger amplitude with more regional details in simulations with 20 km resolution (Figure 5) compared to lower resolution projections (Figure 6). This shows that high-resolution simulations are essential to extract useful regional climate information. The manner of change in precipitation is uneven in ultra-high-resolution models with distinct spatial inhomogeneity (Figure 5). Different factors can contribute to the uneven change in high-resolution grid due to climate warming. The increase in the saturation-specific humidity or the capacity to hold water vapour with the rise in temperature can increase the actual water vapour content in the atmosphere. Thus, if the mean residence time of water vapour in the atmosphere do not change, both precipitation and evaporation would increase with exponential dependence on temperature. But, regional factors which are resolvable with 20 km resolution such as the availability of surface moisture, horizontal convergence/divergence of air flow in the lower atmosphere and orography modulate the concentration of water vapour evaporated from the surface or transported into the area. Thus, the resultant spatial distribution of atmospheric moisture and the precipitation changes can be uneven.

Consistent with the projected changes in summer mean rainfall, the mean annual variations of all-India rainfall in future scenario (Figure 4) also clearly show that intensification of rainfall is projected not only during the summer monsoon but during the rest of the year for most of interior regions. As for the mean rainfall change, the projected future changes suggest suppression of rainfall in May–August with subsequent intensification in September–October for region I and rainfall suppression in June–July for region III.

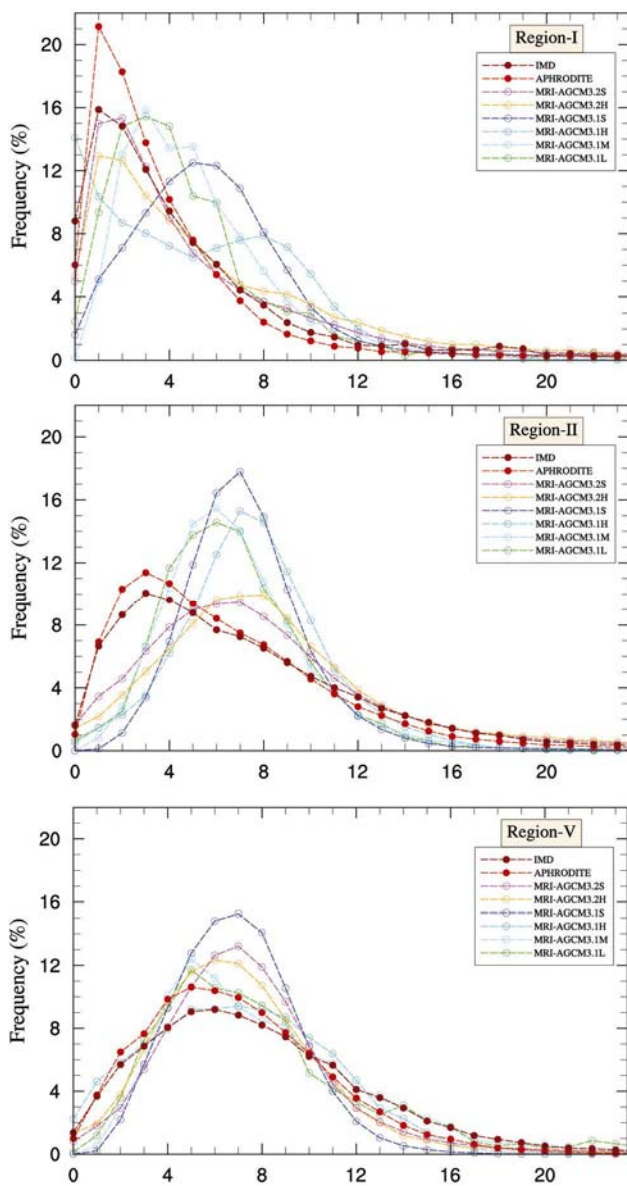


Figure 3. Rainfall–frequency distribution over three homogeneous regions of India (I, II and V) for IMD observation and PDC simulations with different resolutions.

Climate change impact on extreme events

The impact of resolution is typically felt at local or regional scale as a result of interactions between large-scale forcing and local terrain and land surface³; so analysis of climate extremes is especially suited for assessing potential climate change impacts using ultra-high-resolution models. We analyse indices derived from daily maximum temperature and daily precipitation from MRI-AGCM3.2S, MRI-AGCM3.1S and MRI-AGCM3.2H, as recommended by World Meteorological Organization/World Climate Research Programme on Climate Variability and Predictability (WMO/WCRP CLIVAR) Expert Team for Climate Change Detection Monitoring and Indices (ETCCDMI)²⁴ based on indices of occurrence of warm days (TX90p), very wet days (R95p) and extremely wet days (R99p). TX90p represents the warmest decile for maximum temperature and precipitation indices represent rainfall falling above the 95th (R95p) and 99th (R99p) percentiles, which include the most extreme precipitation events. Several studies show that there are

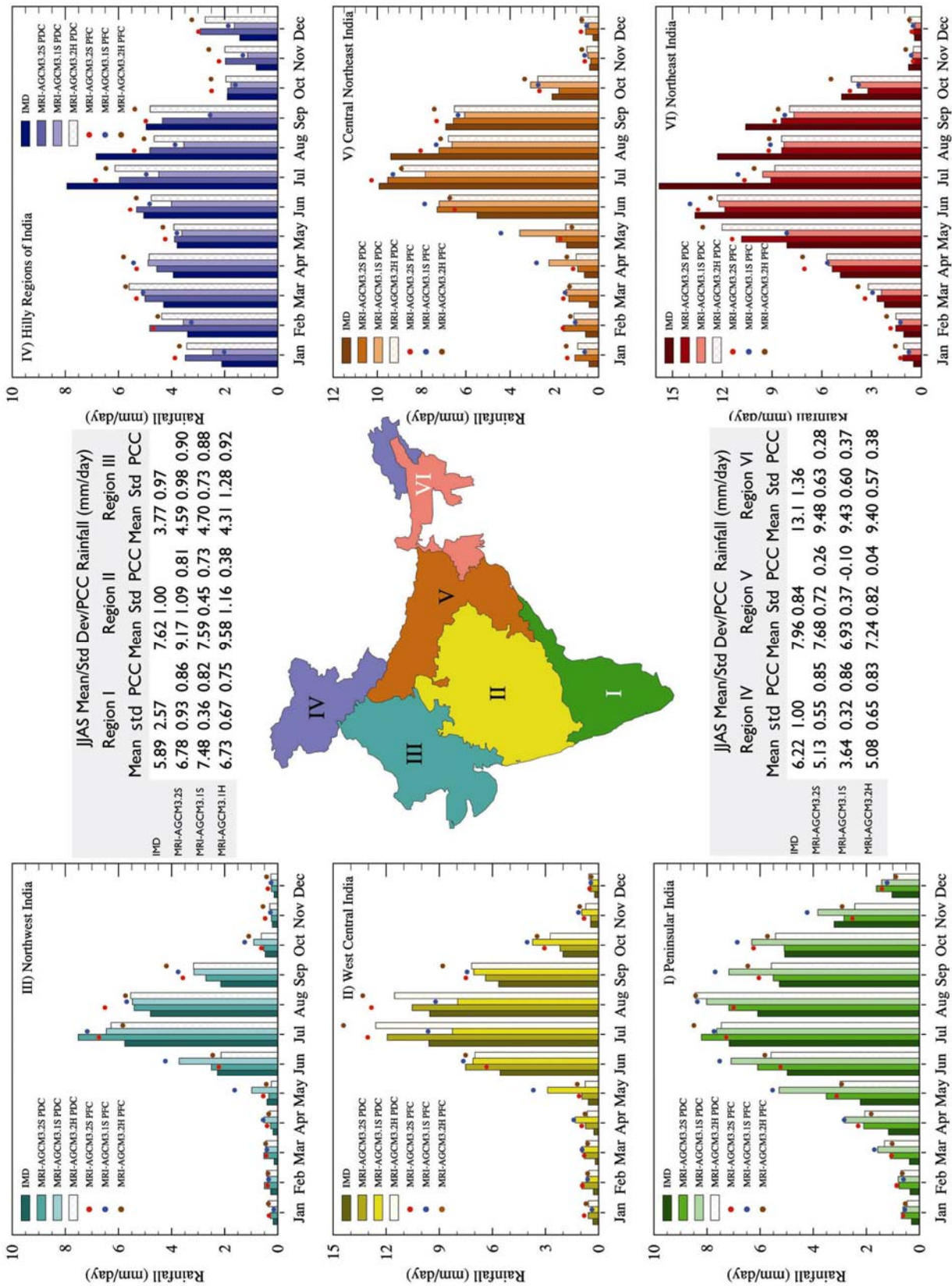


Figure 4. Mean rainfall annual cycle for homogeneous regions of India from IMD observation and PDC and PFC simulations of MRI-AGCM3.2S, MRI-AGCM3.1S and MRI-AGCM3.2H. Observed and simulated mean and standard deviation, and PCC for PDC simulations are given in the tables.

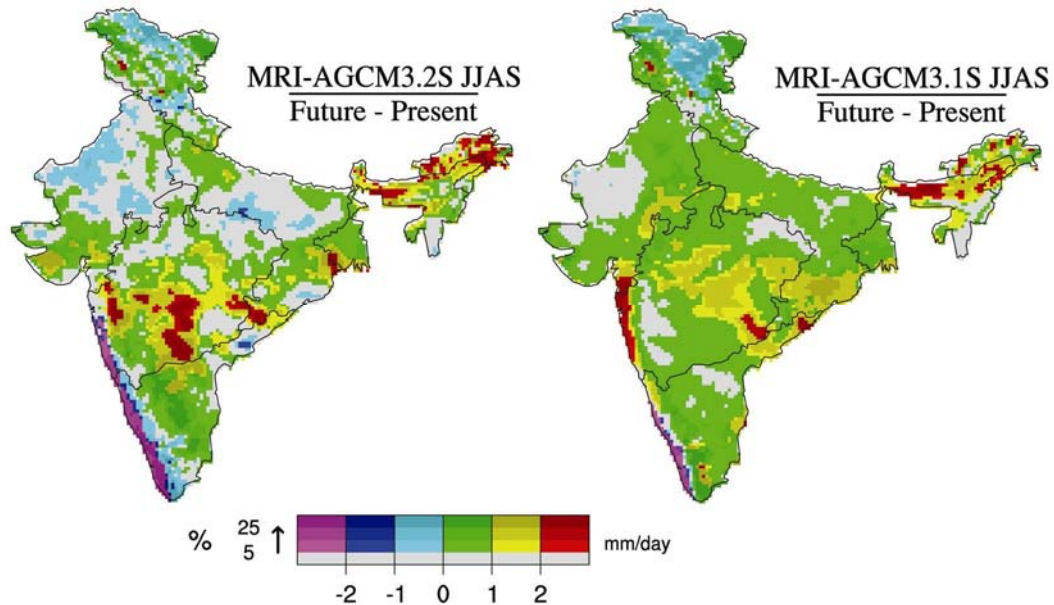


Figure 5. Projected future changes in JJAS mean rainfall over India by MRI-AGCM3.2S and MRI-AGCM3.1S. Within each colour the gradient in hue corresponds to changes as percentage of mean summer monsoon rainfall (<5%: grey, 5–15%, 15–25% and >25%).

positive trends in the frequency of hot events and heavy or in some places reduced precipitation events^{3,17}. However, it is not currently clear in what ways fine-scale feedbacks in high-resolution simulations modulate the regional and local responses to those large-scale changes. Therefore, the impact of warming on the regional distribution of extreme hot and severe precipitation events in India is investigated using ultra-high-resolution projections.

Warm days and hot events

TX90p is defined as the number of days with maximum temperature above 90 percentile value estimated from a base period (PDC simulation). Let TX_{ij} be the daily maximum temperature on day i in period j and $TX_{in,90}$ the calendar day 90th percentile centred on a 5-day window for the base period. The occurrence of warm days is determined where $TX_{ij} > TX_{in,90}$ (ref. 24). During the monsoon season, increase in hot events is not as strong as in March/April (not shown), due to the feedback of widespread increase in future rainfall. Projections indicate that during monsoon (JJAS), the number of warm days and extreme hot events (TX90p) will be increased in future (Figure 7) over the entire country. As seen in the case of the annual cycle of monthly mean temperature, at the end of the 21st century, simulations also predict an increase of maximum temperature (TX_m)²⁴ throughout the year (not shown). Figure 7 also shows the probability density functions (PDFs) for the daily maximum temperature above 90 percentile for JJAS season. PDFs were produced by binning daily maximum temperature above

threshold (90 percentile) during the season for the whole period. The mean and standard deviation of PDC PDF are different from those of PFC simulation, indicating a clear shift towards warmer conditions at the end of the century. Differences between the distributions for the occurrence of warm days in the PDC and future warming climate (PFC) suggest that there will be warming of extreme maximum temperatures in future. The pattern of number of warm days with temperatures greater than 90 percentile in JJAS, appears to have been caused in part by the summer surface-moisture-precipitation feedback in the time-slice experiment⁵.

Rainfall extremes

The patterns of changes in the number of extreme precipitation events (R95p, Figure 8) correspond well to those of seasonal mean precipitation (Figure 5), especially for peaks in frequency over west central and central northeast India, and reduction over the west coast and parts of northwest India and Jammu & Kashmir. The patterns (Figure 5) suggest a weakening of the west coast orographic rain, due in part to the changes in the extreme precipitation regime. In contrast, over west central and central northeast India, positive changes in seasonal mean precipitation were associated with positive changes in the frequency of extreme rainy days (Figure 8). For very heavy precipitation, many coastal areas, except the west coast, exhibit substantial increase in occurrence, with peak positive changes over northern parts of the west coast around Mumbai and east coast^{5,6}. Frequency distribution of daily rainfall above 95 percentile from PDC and

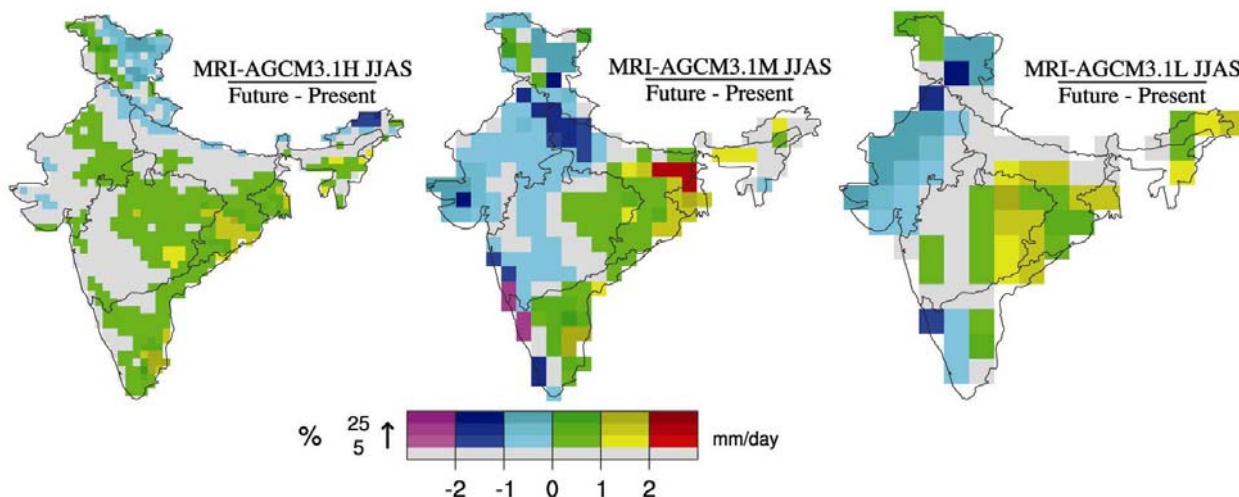


Figure 6. Same as Figure 5, but for MRI-AGCM3.1H, MRI-AGCM3.1M and MRI-AGCM3.1L.

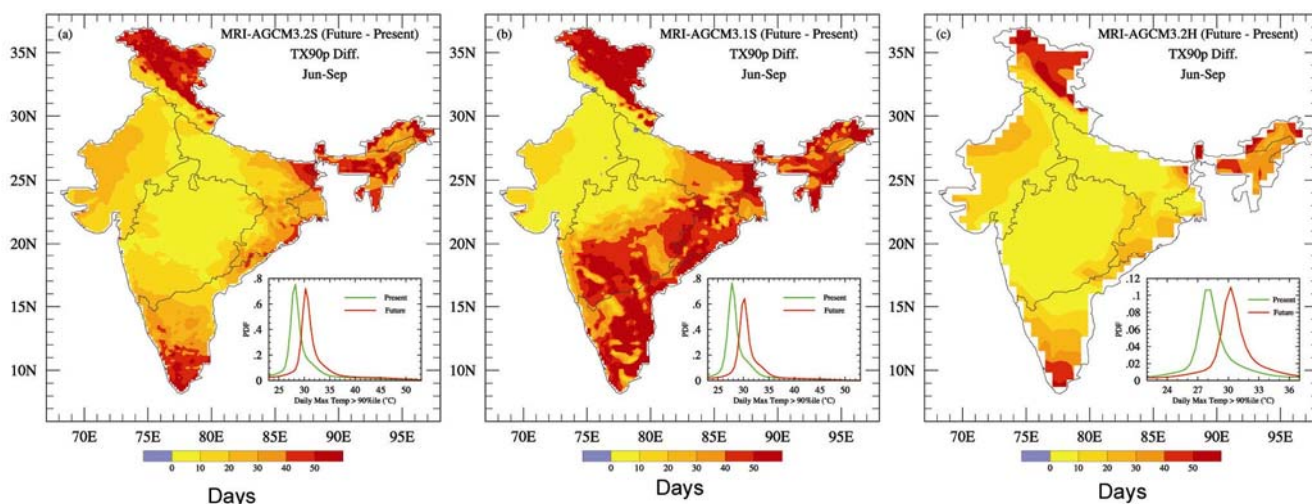


Figure 7. Future changes in number of days in JJAS with daily maximum temperature greater than 90 percentile, between PFC and PDC simulations of MRI-AGCM3.2S, MRI-AGCM3.1S and MRI-AGCM3.2H. (Inset) Probability density functions (PDFs) of daily maximum temperature above 90 percentile in JJAS.

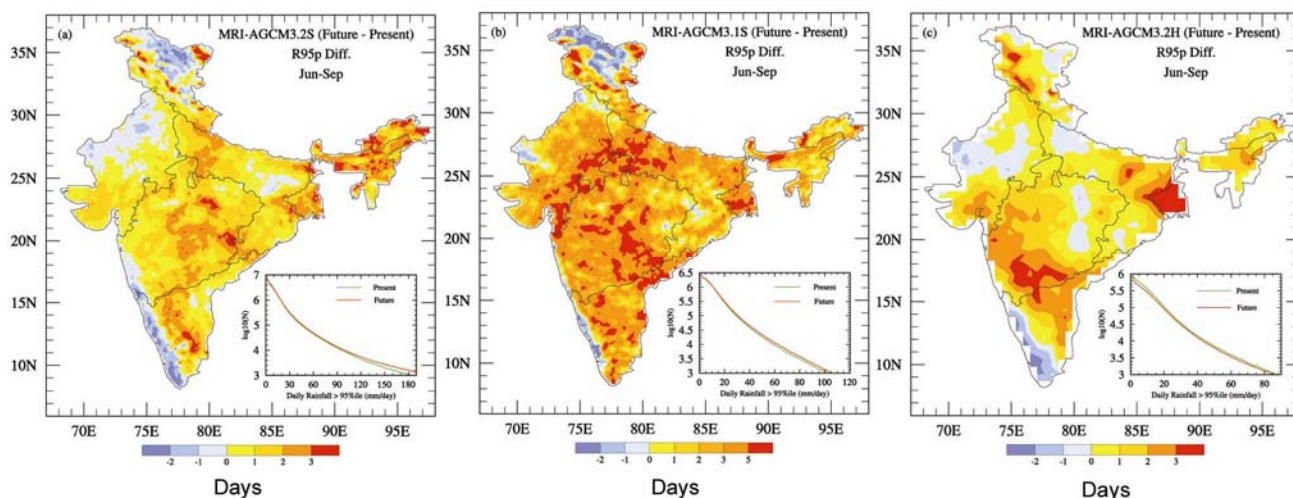


Figure 8. Changes in number of days in JJAS with precipitation greater than 95 percentile between PFC and PDC simulations of MRI-AGCM3.2S, MRI-AGCM3.1S and MRI-AGCM3.2H. Frequency distribution of daily mean precipitation above 95 percentile in JJAS.

PFC simulations is also shown in Figure 8 (inset). Intensification of extreme rainfall events (R99p) also occurs in PFC (not shown).

It is argued that precipitation extremes should increase with global warming^{25–27}. Trenberth *et al.*²⁷ hypothesized that in the PDC, precipitation intensity increases nearly at the same rate as atmospheric moisture^{28,29}, which increases at about 7% K⁻¹ according to the Clausius–Clapeyron equation. They argued that the increase in extreme rainfall could even exceed this rate because additional latent heat released from increased moisture could invigorate the storms. But this does not have to be the case, since the mean static stability of the atmosphere also changes with warming³⁰. An invigorated storm could increase moisture removal from the atmosphere.

On the other hand, global evaporation, which is determined by global surface energy budget, increases at the same rate as global mean precipitation^{31,32}, about 2–3% K⁻¹. This means that in a warmer climate it would take longer for evaporation to replenish atmospheric moisture, thus longer dry spells between storms. Moreover, the enhanced latent heat from convection would make the atmosphere more stable and thus less likely to precipitate, especially for light and moderate precipitation that requires an unstable large-scale environment. For example, over the west coast of India, the resultant effect was found to suppress moderate precipitation due to larger upper tropospheric warming relative to the surface and lower levels⁶.

Concluding remarks

Diagnostics of MRI global climate model simulations at different horizontal and vertical resolutions of T_L959L60, T_L319L60, T_L59L40 and T_L95L40 (~20, 60, 120 and 180 km respectively) illustrates the marked skill of the model in capturing major characteristics of climatological summer monsoon rainfall over India, and frequency distribution of summer rainfall and mean annual variation of rainfall over most of the homogeneous regions, when ultra-high resolution of ~20 km is employed. The model shows consistent further improvement in simulating mean summer monsoon with a new physics scheme for deep convection at high-resolution (20 and 60 km). At 20 km resolution, with recent deep convection schemes, present-day simulation captures the regional details of Indian summer monsoon and compares well with observed precipitation distribution. This indicates that simulation of the local aspects of the Indian summer monsoon benefits from ultra-high resolution. Therefore, we can have better confidence in the validity of the prediction of future changes in Indian summer monsoon on the basis of time-slice experiment.

Future projections using time-slice simulations of very high-resolution models with two deep convection schemes

under global warming scenario show widespread but spatially varying increase in rainfall over the interior regions of peninsular, west central, central northeast and NE India (~5–20%) and significant reduction in orographic rainfall over the west coast (~10–15%, consistent with the recent observed trends) and some parts of hilly regions of Jammu & Kashmir and northwest India (~5%). Over the west coast, the drastic reduction of vertical ascent and weakening of circulation due to upper tropospheric warming effect predominate over the moisture build-up effect (that causes enhanced rainfall over other parts) in reducing the rainfall.

The ultra-high-resolution model projects spatially heterogeneous increase in extreme hot events (highest decile) over the whole of India and increasing trend in the number of warm days. Projected changes in extreme rainfall events show intensification of extreme rainfall over most parts of India by the end of the century, with opposite trend over the west coast for both heavy (above 95 percentile) and extreme (above 99 percentile) rainfall events. The close correspondence between changes in seasonal mean rainfall and extreme rainfall events points out that the contribution of high percentile rainfall events to seasonal rainfall is also likely to increase in future over the country. For the west coast, the increase in temperature, coupled with a decline in rainfall, will have drastic consequences on the production of crops. This will exacerbate existing vulnerabilities of the people who depend on agriculture. On the other hand, decrease of moderate precipitation can lengthen dry spells and increase the risk of drought because light and moderate precipitation is a critical source of soil moisture as well as groundwater. Over other regions, increases in heavy precipitation can increase surface run-off and lead to intense floods and landslides.

Very high-resolution is found to be crucial not only for realistic mean summer monsoon simulation, but for achieving useful future projections of Indian monsoon. At lower resolutions, the simulations fail to capture observed characteristics of present-day monsoon rainfall and its spatial heterogeneity. This warrants consideration that fine-scale processes at sufficiently high-resolution are critical for reasonable probabilistic projection of regional-scale climate change.

The future changes in the seasonal mean monsoon and extreme events predicted by the simulations are plausible considering the capability of the model to simulate these aspects of present-day Indian summer monsoon. However, it is to be noted that this is one of several possibilities to be expected in the future. For example, the projected results can be sensitive to the particular scenario for concentration of the important greenhouse gases (GHGs) in the future. Further, the projection can be sensitive to the initial and boundary conditions used. In order to assess the effects of these uncertainties, an ensemble of global time-slice simulations would have to be performed, with

different ultra-high-resolution climate models, initial and boundary forcing with different GHG scenarios prescribed.

1. Gadgil, S. and Sajani, S., Monsoon simulation in AMIP runs. *Climate Dyn.*, 1998, **14**, 659–689.
2. Meehl, G. A. and Washington, W. M., South Asian summer monsoon variability in a model with a doubled atmospheric carbon dioxide concentration. *Science*, 1993, **260**, 1101–1104.
3. IPCC, Regional climate projections. In *Climate Change 2007: The Physical Science Basis*, W.G.I. contribution to IPCC AR4 (eds Solomon, S. *et al.*), Cambridge University Press, New York, 2007.
4. Turner, A. G. and Slingo, J. M., Uncertainties in future projections of extreme precipitation in the Indian monsoon region. *Atmos. Sci. Lett.*, 2009, **10**, 152–158; doi: 10.1002/asl.223.
5. Rajendran, K. and Kitoh, A., Indian summer monsoon in future climate projection by a super high-resolution global model. *Curr. Sci.*, 2008, **95**, 1560–1569.
6. Rajendran, K., Kitoh, A., Srinivasan, J., Mizuta, R. and Krishnan, R., Monsoon circulation interaction with Western Ghats orography under changing climate: projection by a 20 km mesh AGCM. *Theor. Appl. Climatol.*, 2012, **110**, 555–571.
7. Rajendran, K., Nanjundiah, Ravi, S. and Srinivasan, J., Comparison of seasonal and intraseasonal variation of tropical climate in NCAR CCM2 GCM with two different cumulus schemes. *Meteorol. Atmos. Phys.*, 2002, **79**, 57–86.
8. Mizuta, R. *et al.*, 20 km-Mesh global climate simulations using JMA-GSM model: mean climate states. *J. Meteorol. Soc. Jpn*, 2006, **84**, 165–185.
9. Arakawa, A. and Schubert, W. H., Interaction of a cumulus cloud ensemble with the largescale environment: part I. *J. Atmos. Sci.*, 1974, **31**, 674–701.
10. Randall, D., and Pan, D. M., Implementation of the Arakawa-Schubert cumulus parameterization with a prognostic closure. *Meteorol. Monogr.*, 1993, **46**, 145–150.
11. Hortal, M., The development and testing of a new two-time level semi-Lagrangian scheme (SETTLS) in the ECMWF forecast model. *Q. J. R. Meteorol. Soc.*, 2002, **128**, 1671–1687.
12. Mizuta, R. *et al.*, Climate simulations using MRI-AGCM3.2 with 20-km grid. *J. Meteorol. Soc. Jpn.*, A, 2012, **90**, doi: 10.2151/jmsj.2012-A12, o233-258.
13. Yukimoto, S. *et al.*, Meteorological Research Institute-Earth System Model version 1 (MRI-ESM1): model description, Technical Report of Meteorological Research Institute, Japan, 64, 2011 (available at http://www.mri-jma.go.jp/Publish/Technical/DATA/YOL_64/tec_rep_mri_64.pdf), p. 88.
14. Tiedtke, M., A comprehensive mass flux scheme for cumulus parameterization in large-scale models. *Mon. Weather Rev.*, 1989, **117**, 1779–1800.
15. Nakicenovic, N. and Swart, R., IPCC special report on emission scenarios. In IPCC Working Group I, Cambridge University Press, Cambridge, UK, 2000, p. 599.
16. Rayner, N. A., Parker, D. E., Horton, E. B., Folland, C. K., Alexander, L. V. and Rowell, D. P., Global analyses of SST, sea ice and night marine air temperature since the late nineteenth century. *J. Geophys. Res. Atmos.*, 2003, **108**, 4407; 10.1029/2002JD002670.
17. Endo, H., Kitoh, A., Ose, T., Mizuta, R. and Kusunoki, S., Future changes and uncertainties in Asian precipitation simulated by multiphysics and multi-sea surface temperature ensemble experiments with high-resolution Meteorological Research Institute atmospheric general circulation models (MRI-AGCMs). *J. Geophys. Res.*, 2012, **117**, 17, D16118; doi: 10.1029/2012JD017874.
18. Mizuta, R., Adachi, Y., Yukimoto, S. and Kusunoki, S., Estimation of future distribution of sea surface temperature and sea ice using the CMIP3 multi-model ensemble mean. Technical Report of Meteorological Research Institute, Japan, 2008, 56, p. 28; http://www.mri-jma.go.jp/Publish/Technical /DATA/VOL_56/56_en.html
19. Meehl, G. A. *et al.*, The WCRP CMIP3 multi-model dataset: a new era in climate change research. *Bull. Am. Meteorol. Soc.*, 2007, **88**, 1383–1394; doi: <http://dx.doi.org/10.1175/BAMS-88-9-1383>.
20. Rajeevan, M., Bhate, J., Kale, J. D. and Lal, B., High resolution daily gridded rainfall data for Indian region: analysis of break and active monsoon spells. *Curr. Sci.*, 2006, **91**, 296–306.
21. Yatagai, A., Arakawa, O., Kamiguchi, K., Kawamoto, H., Nodzu, M. I. and Hamada, A., A 44-year daily gridded precipitation dataset for Asia based on a dense network of rain gauges. *SOLA*, 2009, **5**, 137–140.
22. Parthasarathy, B., Munot, A. A. and Kothawale, D. R., Monthly and seasonal rainfall series for all-India homogeneous regions and meteorological subdivisions: 1871–1994. Research Report No. RR-065, Indian Institute of Tropical Meteorology, Pune, 1995, p. 113.
23. Kitoh, A. and Kusunoki, S., East Asian summer monsoon simulation by a 20-km mesh AGCM. *Climate Dyn.*, 2008, **31**, 389–401; doi:10.1007/s00382-007-0285-2.
24. Alexander, L. V. *et al.*, Global observed changes in daily climate extremes of temperature and precipitation. *J. Geophys. Res.*, 2006, **111**, D05109; doi: 10.1029/2005JD006290.
25. Trenberth, K. E., Conceptual framework for changes of extremes of the hydrological cycle with climate change. *Climatic Change*, 1999, **42**, 327–339.
26. Allen, M. R. and Ingram, W. J., Constraints on future changes in climate and the hydrologic cycle. *Nature*, 2002, **419**, 224–232.
27. Trenberth, K. E., Dai, A., Rasmussen, R. M. and Parsons, D. B., The changing character of precipitation. *Bull. Am. Meteorol. Soc.*, 2003, **84**, 1205–1217; doi:10.1175/BAMS-84-9-1205.
28. Bretherton, C. S., Peters, M. E. and Back, L. E., Relationships between water vapour path and precipitation over the tropical oceans. *J. Climate*, 2004, **17**, 1517–1528.
29. Neelin, J., Peters, O. and Hales, K., The transition to strong convection. *J. Atmos. Sci.*, 2009, **66**, 2367–2384.
30. Del Genio, A. D., Yao, M.-S. and Jonas, J., Will moist convection be stronger in a warmer climate? *Geophys. Res. Lett.*, 2007, **34**, L16703.
31. Cubasch, U. and Meehl, G. A., Projections of future climate change. In *Climate Change 2001: The Scientific Basis* (eds Houghton, J. T. *et al.*), Cambridge University Press, Cambridge, UK, 2001, pp. 525–582.
32. Held, I. M. and Soden, B. J., Robust responses of the hydrological cycle to global warming. *J. Climate*, 2006, **19**, 5686–5699.

ACKNOWLEDGEMENTS. We thank Prof. J. Srinivasan, IISc, Bangalore for many useful discussions and suggestions. K.R. was supported by KAKUSHIN programme funded by the Ministry of Education, Culture, Sports, Science and Technology (MEXT), Japan. K.R. and S.S. also thank the Department of Environment and Climate Change, Government of Kerala for a research grant (R-1-166), Collaborative Project R-8-118 and HPC of CSIR-4PI, Bangalore. A.K. was supported by the KAKUSHIN and SOUSEI programmes for collaborations for climate change studies. We also thank Dr R. Mizuta, MRI, Japan for help.